Surface Sorption of Divalent Manganese Ion from Water by Biomass of Date Palm Seeds: Kinetic Studies

MOHAMMED A. AL-ANBER *, [1], IDREES F. AL-MOMANI [2], WALA' AL-QAISI [1]

[1] Department of Chemistry and Industrial Chemistry, Faculty of Sciences, Mu´tah University, P.O.

Box 7, 61710 Al-Karak, JORDAN

[2] Department of Chemistry, Faculty of Sciences, Yarmouk University, Irbid, JORDAN

Abstract: - The biomass of date Palm seeds (DPS) can be utilized for the sorption of Mn(II) ion from the water in the batch sorption process. The kinetics of sorption have been carried out by controlling different parameters such as initial concentration, dosage, temperature, and pH. The sorption equilibrium is achieved during the first 180 minutes. The maximum removal of Mn(II) ion is ca. 100 % upon the study conditions of $C_i = 1$ mg L^{-1}, $T = 35\ ^0C$, 80 rpm, pH = 2, and dosage = 2 g L^{-1}. The reaction kinetic models of pseudo-first-order and pseudo-second-order have been used to describe the sorption rate and mechanism of the Mn(II) ion onto the DPS surface. The kinetic parameters, the rate constant, and sorption capacities have been calculated. The possible sorption mechanism of Mn(II) ion onto the DPS surface is proposed.

Key-Words: - Biomass, Seeds, Manganese ion, Date Palm, Sorption, pseudo-second-order, Kinetic Studies

1 Introduction

Nowadays, the excessive utilization of manganese-containing products, mine waters, steel manufacturing industries leads to environmental pollution. Wherein, manganese is a very common contaminant of wastewater and groundwater occurring with iron. The concentration of Manganese ion in water more than 0.1 mg/l can cause the undesirable taste to beverages and stains plumbing fixtures and laundry. The primary target of manganese health impact is the nervous system, and common symptoms of toxic exposure include ataxia, dementia, anxiety, a 'mask-like' face, and manganese, a syndrome similar to Parkinson's disease. When manganese (II) compounds in solution undergo oxidation, manganese is precipitated, resulting in an encrustation problem [1-2]. The divalent form Mn(II) ion predominates in most water at pH = 4–7, but more highly oxidized forms may occur at higher pH. Both Mn(II) and Mn(VII) are soluble in water while Mn(IV) is not [3].

Various efforts concern in the physicochemical treatment techniques for the removal of heavy metals from wastewaters [4-11]. These techniques are precipitation [12-14], coagulation/ flocculation [15-16], ion-exchange [17], oxidation-filtration [18], electrochemical operations [19-20], biological operations [21], adsorption and membrane processes [22].

The adsorption process is used to remove toxic metal ions and non-degradable nature of metallic species, such as Mn (II) at high concentration level, and chemicals from the water that cannot be treated by conventional treatment methods. The most widely used adsorbent for the treatment of manganese ion of wastewater are polymeric materials [23-29], natural minerals [30] and activated carbon [31]. However, activated carbon is relatively expensive. Therefore, the searching for low-cost adsorbents is a primary concern of the research work .

The industrial wastewater in Jordan coming from the manufacturing of products, especially batteries is initially treated with a plant before disposal of the sewage network, which complies with the sanitation instructions issued by the Jordan Industrial Estate Corporation. The industrial wastewater shall be disposed to the sewage network, providing that the quality of wastewater matches with the characteristics included metal ion active substances such as Mn(II) ion with less than 0.20 mg L-1 [32]. Because of this problem and due to the availability, advantages, and accessibility of *the biomass of date seeds* (DPS) in Middle East countries, it is possible to use BDS for removing Mn(II) ion from aqueous solutions .

To the best of my knowledge, up to date, we do not find any study related to utilize the *biomass of date palm seeds* (DPS) surface as a natural filtering material for removing Mn(II) ion from an aqueous solution. Herein, the kinetic and thermodynamic sorption are carried out by using several models such as pseudo-first-order and pseudo-second-order. Sorption diffusion models, such as Weber-Morris intra-particle diffusion model, have been also used to describe the adsorption rate of the Mn(II) ion onto solid particles of the biomass of date palm seeds. The equilibrium interface between the Mn(II) ion solution and the DPS solid particles of the sorbent can be determined in the condition of the maximum sorbent capacity.

2 Problem Formulation

2.1 Preparation of *Date Palm Seeds* Biomass:

The biomass of the *Date Palm Seeds* (DPS) were obtained locally from Jordan (Jordan Valley region). We have used one type of *date palm seeds* (Mabroum-type) in our experiments. These seeds were washed with distilled water and dried at room temperature. They were washed three times by *n-hexane* and then dried at room temperature. After drying, the DPS were heated in the oven (150 ºC) for three hours to produce *dry biomass of Date Palm Seeds*. They were crushed and ground into powdered form. The powder of the DPS was screened into several size fractions in the range of 150 - 180 µm using standard Tyler screen series. In the present study, physical and chemical treatment was undertaken. However, the major chemical compositions of biomass were lignin and cellulose backbone [33].

2.2 Reagents

All chemicals were used as received. The salt of manganese (II) ion is $MnCl_2.4H_2O$ was purchased from Fluka Chemika. The NaOH and HCl were purchased from Merck. Stock solution (1000 mg L^{-1}) of Mn(II) ion was prepared by dissolving the exact amount of $MnCl_2.4H_2O$ (± 0.01 g) in 1000 mL ultrapure deionized water (18 Ω cm). The standard model solutions of 1-100 mg L^{-1} were prepared by appropriate dilution. The initial pH of the solution was adjusted by using 1.0 M HCl or 1.0 M NaOH solution.

2.3 Apparatus and instruments

Atomic Absorption Spectrophotometer, AAS, (Varian Spectra AA 55) was used to find the concentration of the Mn(II) ion in aqueous solution. The pH of all solutions was recorded by pH meter (Oiron 520). The temperature was controlled using a temperature controller (Gefellschaft Funn 1003, ±0.1 ºC). Isothermal shaker was also used (Gefellschaft Fur 978). The analytical balance is used with ± 0.1 mg (Sartorius, CP324-S/ management system certified according to ISO 9001).

2.4 Equilibrium studies

The sorption of Mn(II) ion was calculated from the mass balance, which was stated as the amount of Mn(II) ion adsorbed onto the biomass of date Palm Seeds. It equals the amount of Mn(II) ion removed from the aqueous solution. Mathematically, it can be expressed by equations 1-2:

$$q_e = \frac{(C_i - C_e)}{S} \tag{1}$$

$$q_t = \frac{(C_i - C_t)}{S} \tag{2}$$

Where, q_e is the Mn(II) ion amount adsorbed on the DPS surface at equilibrium (mg g^{-1}); q_t is the Mn(II) ion amount adsorbed on the DPS surface at a specific time (mg g^{-1}); C_i is the initial concentration of Mn(II) ion in the aqueous solution (mg L^{-1}); C_e is the equilibrium concentration or final concentration of Mn(II) ion in the aqueous solution (mg L^{-1}); and C_t is the final concentration of Mn(II) ion in the aqueous solution (mg L^{-1}) at a specific time, *t*,.

The dosage (slurry), S, the concentration of Mn(II) ion is expressed by equation 3:

$$S = \frac{m}{v} \tag{3}$$

Where v is the initial volume of Mn(II) ion solution used (L) and m is the mass of Mn(II) adsorbent.

The adsorption percentages (%) are calculated by equation 4:

$$\%\, Removal\ of\ Mn(II)ion = \frac{C_i - C_e}{C_i} \times 100\% \tag{4}$$

The simplest and most common method of estimating contaminant retardation is based on the distribution coefficient, K_d. The K_d parameter is a factor related to the partitioning of a contaminant (Mn^{2+} ion) between the solid Mn(II) adsorbent and aqueous phases. The partition coefficient, K_d, is defined as the ratio of Mn(II) ion quantity that adsorbed per mass of Mn(II) to the amount of Mn(II) ion remaining in the solution at equilibrium.

The distribution ratio (K_d) is calculated by using equation 5:

$$K_\mathrm{d} = \frac{\text{Amount of Mn(II) ion in Mn(II)}}{\text{Amount of Mn(II)ion in solution}} \times \frac{1}{\mathrm{S}} \tag{5}$$

Furthermore, the adsorption percentages and K_d (L g^{-1}) are correlated by equation 6 [34]:

$$\% \text{ of Adsorption} = \frac{1000\mathrm{K_d}}{\mathrm{K_d}+\frac{1}{\mathrm{S}}} \qquad (6)$$

3 Problem Solution

3.1 Sorption Kinetic and Diffusion Models

For the kinetic studies, several samples containing 0.1 g DPS and 50 ml of Mn(II) ion solutions (C_i = 100 mg L^{-1}) were placed in the 100 ml flasks. The initial pH was adjusted using 1 M NaOH or 1M HCl solution. These flasks were agitated using a temperature-controlled shaker (study at various T = 25, 35, 45 and 55 °C) at 80 rpm for the sorption period of 1 - 180 minutes and pH$_i$ = 5.4. Afterward, the flasks were removed from the shaker for every 10 minutes in the first 60 minutes and then 30 minutes until the end of 180 minutes. The DPS solid was filtered using filter paper (Whatman No. 41). The filtrate supernatant solutions were analyzed. All the reported results were the average of at least triplicate measurements.

Figure 1 shows the effect of temperatures vs. sorption time. However, at the initial stage, the removal rate of Mn(II) ion is relatively not high during the first 5 minutes. This is due to the poor interaction with the surface based on the selected sorption parameters. The final equilibrium of sorption starts after 90 minutes yielded a maximum removal of ca. 25 %. This finding of trend agrees with the reported kinds of literature [31-42].

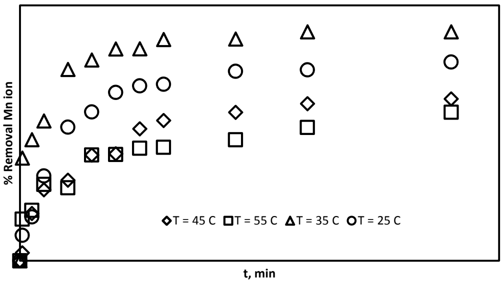

Fig. 1. Effect of temperatures *vs.* sorption time of Mn(II) ion onto DPS, dosage = 2 g L^{-1}, 80 rpm, and C_i =100 mg L^{-1}, pH = 5.4

It is necessary to integrate the rate law (which is given as the time-derivative of one of the concentrations) and the potential rate-controlling steps (such as mass transport and chemical reaction processes) to understand how the concentrations of the Mn(II) ion in a sorption change with time. These kinetic models include the pseudo-first-order, the pseudo-second-order equation, and the Elovich equation.

The pseudo-first-order kinetic model and its integral can be expressed by equation 7 [37-38]:

$$\ln(q_e - q_t) = \ln q_e - k_1 t \qquad (7)$$

Where q_e and q_t (mg g^{-1}) are the amounts of adsorbed Mn(II) ion at equilibrium and at the time (t), respectively, k_1 (min^{-1}) is the pseudo-first-order rate constant, and t (minutes) is contact time. The pseudo-second-order kinetic model and its integral form. This model is expressed by the equation 8 [39-40]:

$$\frac{t}{q_t} = \frac{1}{k_2 q_e^2} + \frac{t}{q_e} \qquad (8)$$

where k_2 is the rate constant of the pseudo-second-order kinetic model(g mg^{-1} min^{-1}). The value of k_2 can be determined by plotting t/q_t versus t to obtain a straight line of slope $1/q_e$ and intercept of $1/(k_2 q_e^2)$. As shown, the values of k_2 and q_e. The correlation coefficient (R^2) of the plot is considered good approval for the results. The degree of goodness of a linear plot can be judged from the value of R^2 of the plot, which can also be regarded as a criterion in the determination of the adequacy of the kinetic model. Furthermore, it is necessary to match the calculated $q_{e\,cal}$ with the experimental $q_{e\,Exp}$ value.

3.2 Kinetic model controlling by Temperature variations:

Figure 2 shows the kinetic model of Pseudo-second order controlling by Temperature variations. From the determination coefficient values R^2 above, the adsorption of Mn(II) ion transport onto the DPS surface is regarded as pseudo-second-order (R^2 = 0.999) rather than pseudo-first-order (R^2 = 0.88 to 0.97) as shown in Figures 2(a-b). It is known that if a kinetic model follows the pseudo-first-order or pseudo-second-order reaction, then the reaction follows physisorption and chemisorption, respectively. This means that the Mn(II) ion can be chemisorption by the coordination Mn(II) ion with the active sites onto the DPS surface. Furthermore, it is found that the calculated $q_{e\,cal}$ matches with the experimental $q_{e\,Exp}$ value as shown in Figure 2c. This result was found matching with the reported literature by utilizing Acid-treated Activated Carbon [42].

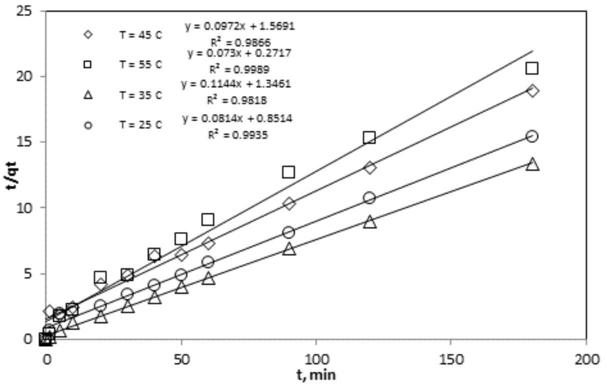

Fig 2a. Pseudo-second-order adsorption model of Mn(II) ion onto DPS particles controlled by variant Temperatures (dosage = 2 g L^{-1}, 80 rpm, and C_i = 100 mg L^{-1}, pH$_i$ = 5.4, T = 25, 35, 45 and 55 ^{0}C).

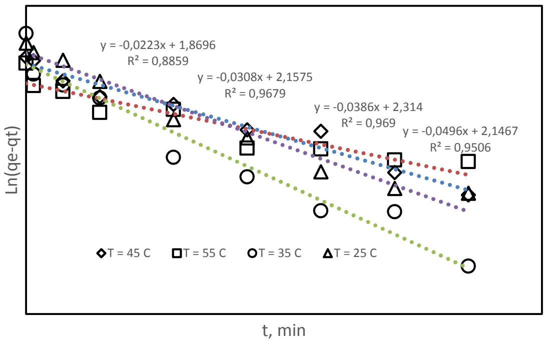

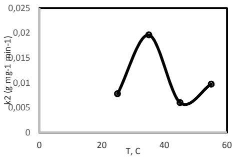

Fig 2b. Pseudo-First-orde Mn(II) ion onto DPS partic variant Temperatures (dosage = 2 100 mg L^{-1}, pH$_i$ = 5.4, T = 25, 35, 45 and 55 ^{0}C).

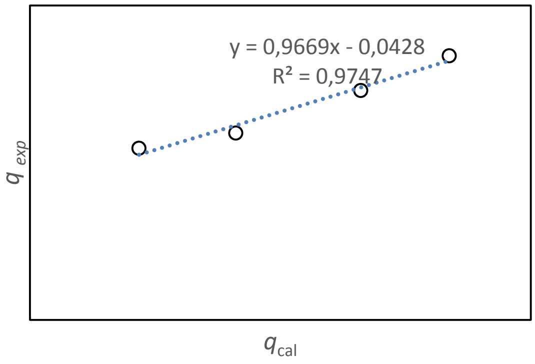

Fig. 2c. Plot of q_{exp} *vs.* q_{cal} related to the Pseudo-Second-order adsorption model of Mn(II) ion onto DPS particles controlled by variant Temperatures (dosage = 2 g L^{-1}, 80 rpm, and C_i = 100 mg L^{-1}, pH$_i$ = 5.4, T = 25, 35, 45 and 55 ^{0}C).

Table 1. The parameters of the Pseudo-second-order adsorption model of Mn(II) ion onto DPS particles controlled by variant Temperatures

T, ^{0}C	k_2 (g mg^{-1} min^{-1})	$q_{e,\,Exp}$ (mg g^{-1})	$q_{e,\,Calc}$ (mg g^{-1})	x^2	R^2
25	0.007782	11.67	12.28501	0.050062	0.9935
35	0.019614	13.445	13.69863	0.018515	0.9818
45	0.006021	9.508197	10.28807	0.075803252	0.9989
55	0.009722	8.729508	8.741259	0.001344285	0.9866

$$x^2 = \frac{q_{cal} - q_{exp}}{q_{cal}}$$

3.3 Kinetic model controlling by pH variations:

Figure 3 shows the effect of pH *vs.* sorption time. However, at the initial stage, the removal rate of Mn(II) ion is relatively not high during the first 5 minutes. This is due to the poor interaction with the surface based on the selected sorption parameters. The final equilibrium of sorption starts after 90 minutes yielded a maximum removal of ca. 25 %, 15 % and 2 % for pH = 5.4, 7 and 2, respectively. Furthermore, it is found that the calculated q_{cal} matches with the experimental q_{exp} value as shown in the Table 2. These observations on the results are consistent with reported work [42-46].

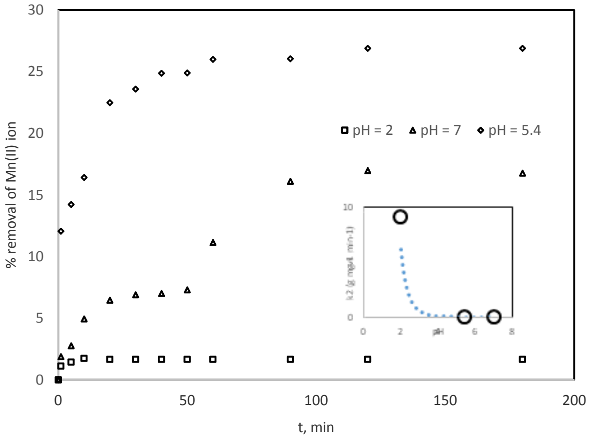

Fig. 3. Effect of temperatures *vs.* sorption time of Mn(II) ion onto DPS, dosage = 2 g L^{-1}, 80 rpm, and C_i =100 mg L^{-1}, T = 35 ^{0}C.

Figure 4 shows the kinetic model of pseudo-second-order adsorption model of Mn(II) ion onto DPS particles controlled by variant temperatures. From the determination coefficient values that appeared in Table 2, the adsorption of Mn(II) ion transport onto the DPS surface is regarded as pseudo-second-order rather than pseudo-first-order as shown in Figure 4. This means that the Mn(II) ion can be chemisorbed by the sorption sites onto the DPS surface as shown in Scheme 2. This result was found matching with the reported for the Rice (Oryza sativa) Husk, Esterified Saw Dust, Acid-treated Activated Carbon, Solid Wastes of Sugar

Industry, Sugarcane Bagasse and Activated Carbon [42-46].

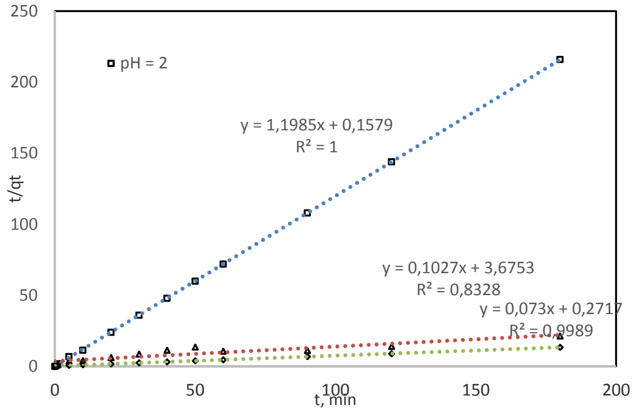

Fig 4. Pseudo-second-order adsorption model of Mn(II) ion onto DPS particles controlled by variant pH influence (dosage = 2 g L^{-1}, 80 rpm, and C_i = 100 mg L^{-1}, T = 35 ^{0}C).

Table 2. The parameters of the pseudo-second-order kinetic model controlling by pH variations

pH	k_2 (g mg^{-1} min^{-1})	$q_{e,\ Exp}$ (mg g^{-1})	$q_{e,\ Calc}$ (mg g^{-1})	x^2	R^2
2	9.096911	0.833333	0.834376	0.00125	1
5.4	0.00287	8.383893	9.737098	0.138974	0.8328
7	0.019614	13.445	13.69863	0.018515	0.9989

3.4 Kinetic model controlling by initial concentration variations:

Figure 5 shows the effect of the initial concentration of Mn(II) ion vs. sorption time. However, at the initial stage, the removal rate of Mn(II) ion is relatively high during the first 5 minutes. It indicates the presence of interaction affinity of Mn(II) ion with the surface based on the selected sorption parameters. Furthermore, it is found that the calculated q_{cal} matches with the experimental q_{exp} value as shown in Table 3. This is due to the availability of active sites, which saturated after 40 minutes of achieving the equilibrium.

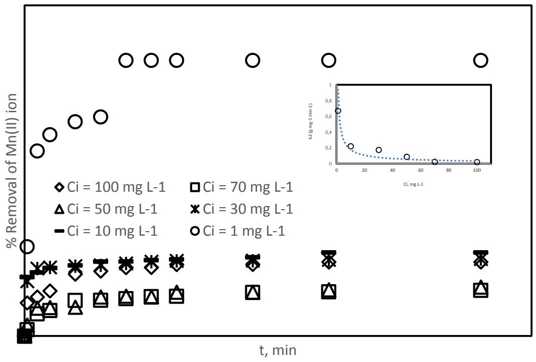

Fig. 5 Effect of temperatures *vs.* sorption time of Mn(II) ion by using DPS, dosage = 2 g L^{-1}, 80 rpm, and C_i =1-100 mg L^{-1}, T = 35 ^{0}C.

Figure 6 shows the Pseudo-second-order adsorption model of Mn(II) ion onto DPS particles controlled by variant initial concentration. From the determination coefficient values that appeared in Table 3, the adsorption of Mn(II) ion transport onto the DPS surface is regarded as pseudo-second-order rather than pseudo-first-order as shown in Figure 6. This means that the Mn(II) ion can be chemisorption by the sorption sites onto the DPS surface as shown in Scheme 2. This result was found matching with the reported results by Rice (Oryza sativa) Husk, Esterified Saw Dust, Acid-treated Activated Carbon, Solid Wastes of Sugar Industry, Sugarcane Bagasse and Activated Carbon [42-46].

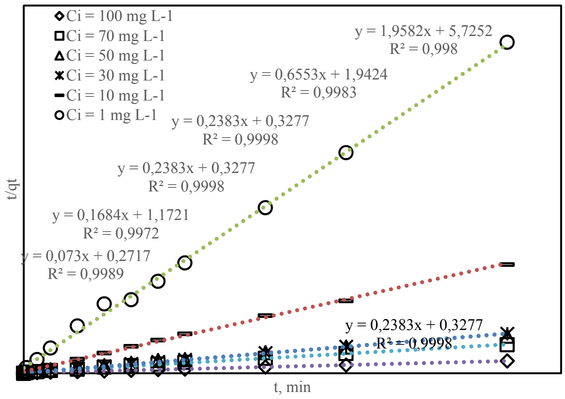

Fig 6a. Pseudo-second-order adsorption model of Mn(II) ion onto DPS particles controlled by the variant initial concentration (dosage = 2 g L^{-1}, 80 rpm, and *pH* = 5.4-5.8, T = 35 ^{0}C).

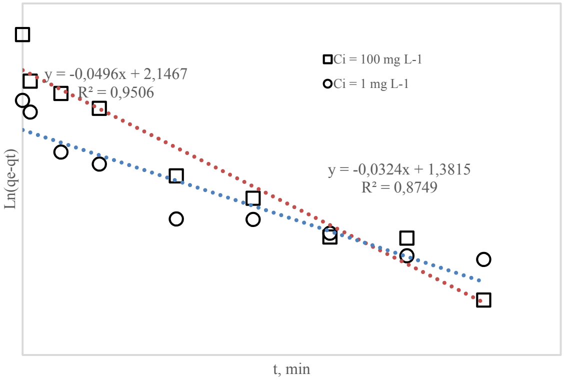

Fig 6b. Pseudo-First-order adsorption model of Mn(II) ion onto DPS particles controlled by the variant initial concentration (dosage = 2 g L^{-1}, 80 rpm, and *pH* = 5.4-5.8, T = 35 ^{0}C).

Table 3. The parameters of the pseudo-second-order adsorption model of Mn(II) ion onto DPS particles controlled by variant initial concentration

Ci mg L^{-1}	**k_2 (g mg^{-1} min^{-1})**	**$q_{e,\ Exp}$ (mg g^{-1})**	**$q_{e,\ Calc}$ (mg g^{-1})**	**x^2**	**R^2**
1	0.669767	0.5000	0.51070	0.0209	0.9980
10	0.221076	1.5190	1.52607	0.0046	0.9983
30	0.173289	4.1870	4.19639	0.0023	0.9998
50	0.086538	4.4450	5.93824	0.2514	0.9998
70	0.024195	5.8010	5.93824	0.0230	0.9972
100	0.019614	13.445	13.6986	0.0185	0.9989

$$x^2 = \frac{q_{cal} - q_{exp}}{q_{cal}}$$

Indeed, the sorption reaction is determined to be chemisorption based on the kinetic processes, which is described well by a pseudo-second-order model. Furthermore, it is necessary to match the calculated q_{cal} with the experimental q_{exp} value. However, a good agreement between the experimental data and the pseudo-second-order model does not mean a proof that the sorption is happened due to chemical reaction between the Mn(II) ion and the active sites in the DPS solids. Therefore, the chemisorption mechanism may be proved more by estimating the activation energies. This activation energy is estimated based on the experiments that carried out at different temperatures.

The activation energy, E_a, is the minimum energy molecules must possess in order to react to form a product. The dependence of adsorption rate constant of an adsorption on temperature can be expressed by the Arrhenius equation 9 [41]:

$$\ln k_2 = \ln A - \frac{E_a}{RT} \qquad (9)$$

Where E_a is the activation energy of the adsorption (kJ·mol^{-1}), R the gas constant (8.314 J·mol^{-1}·K^{-1}), T the absolute temperature (^0K) and e the base of the natural logarithm scale. The quantity A represents the collision frequency and is called the frequency factor. It can be treated as a constant for a given reacting system over a wide temperature range. The Arrhenius plot is obtained by plotting the $\ln k_2$ (k= rate constant) versus the inverse temperature, 1/T as shown in Figure 7. The slope of the *Arrhenius* plot can be used to find the activation energy, E_a.

The resulting sloped line is equal to the negative activation energy E_a (= + 66.944 kJ. mol^{-1}) divided by the gas constant, R. The positive activation energy is here associated with overcoming the energy barrier of chemical bond formation between the manganese ion and the DPS surface.

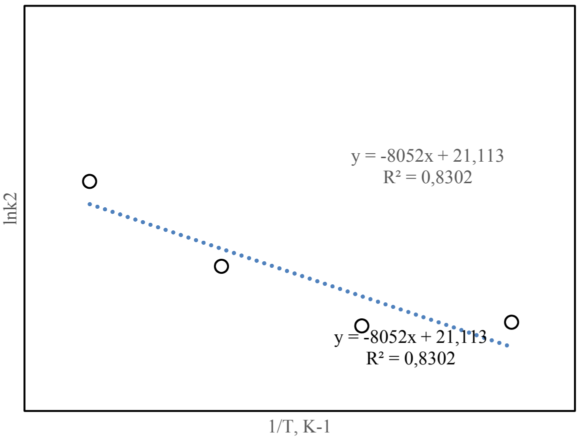

Fig. 7. The activation energy generated from the experimental data of sorption Mn(II) that carried out at different temperatures.

3.5 Sorption Diffusion Models

The pseudo-first-order and pseudo-second-order kinetic models could not identify the diffusion mechanism. Thus, the diffusion of the Mn(II) ion into the DPS surface can be determined by Weber-Moris intraparticle diffusion model [43]. This model was used in the form of equation 14:

$$q_t = k_{int}\sqrt{t} + C \qquad (14)$$

Where C is constant, q_t the amount of Mn(II) ion adsorbed at the time (mg g^{-1}) and k_{int} is the intraparticle diffusion rate constant (mg g^{-1} $min^{\frac{1}{2}}$). A plot of q_t *vs.* $\sqrt{t}$ gives straight-line confirms intraparticle diffusion sorption as shown in Figure 8. Due to the plot is not linear, and *moreso* do not pass through the origin, then intraparticle diffusion could not be the only mechanism involved. Therefore, such a plot, presents multi-linearity, which indicates that three steps have occurred. The first, the gradual adsorption stage (from 0 up to 5 minutes of adsorption period) is the external surface adsorption or instantaneous adsorption stage. The second portion is the sharper portion stage (from 5 up to 50 minutes of adsorption period), where the intraparticle diffusion is rate-controlled (k_{int} = 0.0341 mg g^{-1} $min^{\frac{1}{2}}$ and R^2 = 0.9284, see Fig. 8). The third portion is the final equilibrium stage where the intraparticle diffusion starts (t > 50 min) to slow down due to extremely low solute concentrations in the solution.

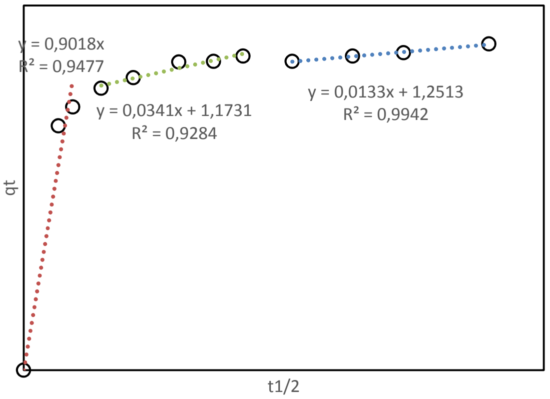

Figure 8. Weber-Moris intra-particular diffusion kinetic model at C_i = 1 mg L^{-1}, Dosage = 2 g L^{-1}, T = 35 ^{0}C and pH$_i$ = 5.9.

4 Conclusion

The biomass of date palm Seeds (DPS) is found to be a very effective adsorbent for the removal of low concentration of the manganese (II) ion from water. The maximum removal has been found 100 % by applying the experimental parameters of low concentration of Mn(II) ion solution (C$_i$ = 1 mg L^{-1}) at the dosage = 2 g L^{-1}, 80 rpm, and C_i =100 mg L^{-1}, T = 35 ^{0}C. The sorption equilibrium can be reached within the first 60 minutes.

The sorption of Mn(II) ion onto DPS is determined to be chemisorption based on the kinetic studies that well described by a pseudo-second-order model, a good agreement between the calculated $q_{e\ cal}$ with the experimental $q_{e\ Exp}$ value and the estimating positive activation energy. This also can be confirmed by the Weber-Moris intraparticle diffusion model, wherein the intraparticle diffusion is rate-controlled sorption reaction.

References:

[1] J.K. Edzwald, WATER Quality and Treatment: *A Handbook on Drinking Water*. 6th Ed., American Water Works Association. McGraw Hill, (2011).

[2] WHO, Manganese in Drinking-water, *Background document for development of WHO Guidelines for Drinking-water Quality*, (2011).

[3] ATSDR. Toxicological profile for manganese. Atlanta, GA, United States Department of Health and Human Services, Public Health Service, Agency for Toxic Substances and Disease Registry, (2000).

[4] M.A. Barakat, New trends in removing heavy metals from industrial wastewater, *Arabian Journal of Chemistry*, **4,** 361-377, (2011).

[5] F. Fu, Qi Wang, Removal of heavy metal ions from wastewaters: A review, *Journal of Environmental Management*, **92**, 407-418 (2011).

[6] T. A. Kurniawan, G.Y.S. Chan, Wai-Hung Lo, S. Babel, Physico–chemical treatment techniques for wastewater laden with heavy metals, *Chemical Engineering Journal*, **118**, 83–98 (2006).

[7] D. Purkayastha, U. Mishra, S. Biswas, A comprehensive review on Cd(II) removal from aqueous solution, *Journal of Water Process Engineering,* **2,** 105–128 (2014).

[8] V. Coman, B. Robotin, P. Ilia, Nickel recovery/removal from industrial wastes: A review, Resour. Conserv. Recy., **73**, 229– 238 (2013)

[9] D. Mohan, C.U. Pittman Jr., Arsenic removal from water/wastewater using adsorbents—A critical review, *Journal of Hazardous Materials*, **142**, 1–53 (2007).

[10] T.M. Alslaibi, I**.** Abustan, M.A**.** Ahmad, A.A**.** Foul**,** Comparison of activated carbon prepared from olive stones by microwave and conventional heating for iron (II), lead (II), and copper (II) removal from synthetic wastewater, *Environmental Progress & Sustainable Energy*, **33** (4), 1074-1085. (2014)

[11] W. W. Eckenfelder, *Industrial Water Pollution Control*, McGraw-Hill, 2000, p.151.

[12] F. Woodard, *Industrial Waste Treatment Handbook*, Butterworth–Heinemann, 2001, p.219.

[13] W. Zhang, C. Cheng, Manganese metallurgy review. Part II: Manganese separation and recovery from solution, *Hydrometallurgy*, **89**, 160–177 (2007).

[14] A.M. Silva, E.C. Cunha, F.D.R. Silva, V.A. Leão, Treatment of high-manganese mine water with limestone and sodium carbonate, *Journal of Cleaner Production*, **29-30**, 11-19 (2012).

[15] X. Tang, H. Zheng, H.Teng, Y. Sun, J.Guo, W.Xiea , Q. Yang, W.Chen, Chemical coagulation process for the removal of heavy metals from water: a review, *Desalination Water Treatment*, 1–16 (2014).

[16] H. Polata, D. Erdogan, Heavy metal removal from waste waters by ion flotation, *Journal of Hazardous Materials*, **148**, 267–273 (2007).

[17] O.N. Kononova, G.L. Bryuzgina, O.V. Apchitaeva, Y.S. Kononov, Ion exchange

recovery of chromium (VI) and manganese (II) from aqueous solutions, *Arabian Journal of Chemistry*, (2015).

[18] D. Ellis, C. Bouchard, G. Lantagne, Removal of iron and manganese from groundwater by oxidation and microfiltration, *Desalination*, **130**, 255-264 (2000).

[19] A. Shafaei, M. Rezayee, M. Arami, M. Nikazar, Removal of Mn^{2+} ions from synthetic wastewater by electrocoagulation process, *Desalination*, **260**, 23–28 (2010).

[20] M. Ince, Treatment of manganese-phosphate coating wastewater by electrocoagulation, *Separation Science and Technology*, **48**, 515–522 (2013).

[21] V. K. Gupta, P.J.M. Carrott, M.M.L. Ribeiro Carrott, Suhas, Low-Cost Adsorbents: Growing Approach to Wastewater Treatment—a Review, *Environmental Science & Technology*, **39**:10, 783-842 (2009).

[22] Deepti S.Patil, Sanjay M.Chavan, John U.Kennedy Oubagaranadin, A review of technologies for manganese removal from wastewaters, *Journal of Environmental Chemical Engineering*, **4**:1, 468-487 (2016).

[23] K.Z. Al-Wakeel, H. Abd El Monem, M.M.H. Khalil, Removal of divalent manganese from aqueous solution using glycine modified chitosan resin, *Journal of Environmental Chemical Engineering*, **3,** 179–186 (2015).

[24] E.A. Moawed, N. Burham, M.F. El-Shahat, Separation and determination of iron and manganese in water using polyhydroxyl polyurethane foam, *Journal of the Association of Arab Universities for Basic & Applied Sciences,* **14**, 60 –66 (2013).

[25] Z. Abdeen, S.G. Mohammad, M.S. Mahmoud, Adsorption of Mn (II) ion on polyvinyl alcohol/chitosan dry blending from aqueous solution, *Environmental Nanotechnology, Monitoring and Management*, **3,** 1–9 (2015).

[26] R. Xu, G. Zhou, Y. Tang, L. Chu, C. Liu, Z. Zeng, S. Luo, New double network hydrogel adsorbent: Highly efficient removal of Cd(II) and Mn(II) ions in aqueous solution, *Chemical Engineering Journal*, **275**, 19-188 (2015)

[27] M.H. Qomi, H. Eisazadeh, M. Hosseini, H.A. Namaghi, Manganese removal from aqueous media using polyanilinenanocomposite coated on wood sawdust, *Synthetic Metals*, **194**, 153–159 (2014).

[28] N.A. Reiad, O.E.A. Salam, E.F. Abadir, F.A. Harraz, Adsorptive removal of iron and manganese ions from aqueous solutions with microporous chitosan/polyethylene glycol blend Membrane, *Journal of Environmental Sciences*, **24** (8), 1425–1432 (2012).

[29] B. Guan, W. Ni, Z. Wu, Y. Lai, Removal of Mn(II) and Zn(II) ions from flue gas desulfurization wastewater with water-soluble chitosan, *Separation and Purification Technology*, 65, 269–274 (2009).

[30] V.J. Inglezakis, M.K. Doula, V. Aggelatou, A.A. Zorpas, Removal of iron and manganese from underground water by use of natural Minerals in batch mode treatment, *Desalination Water Treatment*, **18**, 341–346 (2010).

[31] Abdessalem Omri, Mourad Benzina, Removal of manganese(II) ions from aqueous solutions by adsorption on activated carbon derived a new precursor: Ziziphus spina-christi seeds. *Alexandria Engineering Journal*, **51**, 343–350 (2012).

[32] WHO, A compendium of standards for wastewater reuse in the Eastern Mediterranean Region, 2006

[33] Mohammed A. Al-Anber, Ahmed Abu-Rayyan, Mohammed S. Almogbel, Removal of Inorganic Ferric Ion from Water by using Coal of Date Palm Seeds (CDPS). *Biointerface research in Applied Chemistry*, **6**(2), 1149-1156 (2016).

[34] S. Radi, S. Tighadouini, M. Bacquet, S. Degoutin, F. Cazier, M. Zaghrioui, and Y.N. Mabkhot, Organically modified silica with pyrazole-3-carbaldehyde as a new sorbent for solid-liquid extraction of heavy metals. *Molecules*, **19**, 247 (2014)

[35] Langmuir, I. The Adsorption of Gases on Plane Surface of Glass, Mica and Olatinum. *Journal of the American Chemical Society*, **40**, 1361-1403, (1918).

[36] H. M. F. Freundlich, “Uber Die Adsorption in Losungen, *Zeitschrift fur Physikalische Chemie*,” Leipzig, 57A, 1906, 385-470.

[37] S. Lagergren, Zur theorie der sogenannten adsorption gelöster stoffe. Kungliga Svenska Vetenskapsademiens, *Handlingar*, 24, 1-39 (1898).

[38] Wong Y C, Szeto Y S, Cheung W H, McKay G. Pseudo-first-order kinetic studies of the sorption of acid dyes onto chitosan. *Journal of Applied Polymer Science*, 2004, **92**(3): 1633–1645

[39] Ho Y S, McKay G. The kinetics of sorption of divalent metal ions onto sphagnum moss peat. *Water Research*, 2000, 34(3): 735–742

[40] Y.S. Ho, A.E. Ofomaja, Pseudo-second-order model for lead ion sorption from aqueous solutions onto palm kernel fiber, *Journal of Hazardous Materials*. **129** (2006) 137–142.

[41] P. W. Atkins, and J. De Paula. *Physical Chemistry for the Life Sciences*. New York, Oxford University Press; Freeman. (2006)

[42] J. Singh, N. Dhiman & N. K. Sharma. Effect of Fe(II) on the Adsorption of Mn(II) from Aqueous Solution Using Esterified Saw Dust: Equilibrium and Thermodynamic Studies, *Indian Chemical Engineer*, **60**:3, 255-268 (2018)

[43] W. J. Weber, J. C. Morris, Kinetics of adsorption on carbon from solution, *Journal of the Sanitary Engineering Division*, **89**:2, 31–60 (1963).